Applied Surface Science 287 (2013) 135–142

Contents lists available at ScienceDirect

Applied Surface Science

journal homepage: www.elsevier.com/locate/apsusc

Enhanced visible-light activity of F-N co-doped TiO_2 nanocrystals via nonmetal impurity, Ti^{3+} ions and oxygen vacancies

Guidong Yang[a,*], Ting Wang[a], Bolun Yang[a], Zifeng Yan[c], Shujiang Ding[b,**], Tiancun Xiao[d,***]

[a] Department of Chemical Engineering, School of Chemical Engineering and Technology, Xi'an Jiaotong University, Xi'an 710049, China
[b] Department of Applied Chemistry, School of Science, Xi'an Jiaotong University, Xi'an 710049, China
[c] State Key Laboratory for Heavy Oil Processing, China University of Petroleum, Qingdao 266555, China
[d] Department of Chemistry, Inorganic Chemistry Laboratory, University of Oxford, Oxford OX1 3QR, UK

ARTICLE INFO

Article history:
Received 20 July 2013
Received in revised form
11 September 2013
Accepted 15 September 2013
Available online 21 September 2013

Keywords:
Co-doping
TiO_2
Visible-light-active
ESR
Ti^{3+} ions
Oxygen vacancies
Photodegradation

ABSTRACT

A visible light active F-N co-doped TiO_2 photocatalysts with varying molar ratio of TiO_2/NH_4F were successfully prepared using an effective yet simple ethanol–water solvothermal method. The photocatalytic activities of the prepared catalysts were tested for the degradation of methylene blue (MB) under visible light irradiation. Superior photocatalytic activity relative to that of undoped TiO_2 was observed on the F-N co-doped catalyst with TiO_2:NH_4F molar ratio of 1.0. Based on the characterization results including FT-IR, XRD, Raman analysis, UV–vis DRS, XPS and ESR, the F and N dopants were effectively incorporated into the anatase TiO_2 lattice, and resulted in a decrease in the energy gap, especially for the TONF-2 sample, which shows two optical absorption edge at 2.32 eV and 2.99 eV, respectively. The ESR data showed that the presence of fluorine and nitrogen in the lattice induces the formation of reduced Ti^{3+} centers and oxygen vacancies. In addition, the surface $O_2^{\bullet-}$ radicals were also detected by ESR analysis, which together with $^{\bullet}OH$ radicals are responsible for the MB solution decoloration under visible light. According to the experimental results, it is believed that the enhanced visible light activity arises from the synergistic effect of F-N co-doping, the presence of Ti^{3+} centers and oxygen vacancies, and thus possible mechanism for both visible light absorption and charge separation were proposed.

1. Introduction

Contamination of soil and groundwater from textile dyes and other industrial waste effluent is a serious health and environmental problem [1], and numerous processes have been investigated for treating such pollutants [2]. Among them, photocatalytic oxidation of toxic organic compounds by semiconductors in water and air has received much attention as a promising technology for pollution abatement [3–5]. Titanium dioxide (TiO_2), as one of the most suitable semiconductor for widespread applications in the field of environmental purification, solar energy conversion and hydrogen generation, has attracted extensive interests in the past decade [6–8]. Particularly, the nano-scale titania catalysts, which are the subject of intensive research due to the novel properties and functions associated with individual nanoparticles [9]. However, the nano-structured TiO_2 can only be excited by irradiation under UV light, which accounts for less than 5% of the incoming solar energy [10,11]. Therefore, the search and study for efficient, stable, low-cost and visible-light responsive TiO_2 photocatalyst for environmental protection and energy supply has been an increasingly important research field.

To date, a variety of technologies such as noble metal loading [12], metal ion doping [13], nonmetal doping [3,14–17] and incorporation of electron-accepting materials [18] was developed to expand the visible light absorption and enhance the photocatalytic performance of TiO_2. Among various modification strategies, the nonmetal doping, especially the co-doping TiO_2 with two nonmetal elements has been frequently employed for achieving visible photocatalysts because the co-doping method could effective modify the TiO_2 electronic band gap and accelerate the electron–hole separation [15,16,19]. In this way, the absorption edge of TiO_2 could be red-shifted to higher wavelengths, and leading to the great improvement of photocatalytic activity of TiO_2 under visible light irradiation. Several authors have reported that the co-doping by nitrogen and fluorine is one of the most effective ways for the enhanced quantum efficiency of TiO_2, and the formation of two isolated impurities states after co-doping may

* Corresponding author. Tel.: +86 29 82663189.
** Corresponding author.
*** Corresponding author.
E-mail addresses: guidongyang@mail.xjtu.edu.cn (G. Yang), dingsj@mail.xjtu.edu.cn (S. Ding), Xiao.tiancun@chem.ox.ac.uk (T. Xiao).

0169-4332/$ – see front matter © 2013 Elsevier B.V. All rights reserved.
http://dx.doi.org/10.1016/j.apsusc.2013.09.094

trap the photo carriers and significantly inhibit the recombination of photo-generated electron and holes [15,16,20]. Giannakas et al. [21] reported that the N-F co-doped TiO_2 catalysts prepared by a sol–gel method using NH_4F as N and F dopant precursors, and the obtained samples showed enhanced absorption at visible wavelengths. Huo et al. [15] found that the N and F co-doped TiO_2 photocatalysts prepared by treating the TiO_2 in NH_4F/ethanol fluid under supercritical conditions exhibited very high activity during photocatalytic degradation of MB under visible light irradiation, which was attributed to the synergetic effects between doped N and F. Chen et al. [22] used a facile method of $(NH_4)_2TiF_6$ pyrolysis to prepare nitrogen and fluorine co-doped TiO_2 nanoparticles (N-F-TiO_2). The photocatalytic activity of the obtained N-F-TiO_2 samples was evaluated by the degradation of methylene blue under visible light, and all the samples exhibited much higher photocatalytic activity than P25. These studies showed that the nature of the preparation method exerts an important effect on the catalytic performance of F-N co-doped TiO_2. Therefore, it is interesting to develop a simple, appropriate and efficient method to prepare F-N co-doped TiO_2 catalyst.

Herein, we report an effective yet simple ethanol–water solvothermal method to synthesize pure anatase TiO_2 co-doped nitrogen and fluorine and evaluate their performance in the photodecomposition of methylene blue under visible light irradiation. The degrees of nitrogen and fluorine doping and visible light active mechanism have also been discussed. Furthermore, a variety of characterization techniques have been employed to systematically study the crystal structure, optical absorption and surface property of the as-prepared F-N co-doped TiO_2.

2. Experiment

2.1. Synthesis

F-N co-doped TiO_2 samples were synthesized using ethanol–water solvothermal method. In a typical procedure, 0.01 mol $Ti(OBu)_4$ was dispersed into 30 mL of absolutely ethanol containing 1 mL acetic acid, this solution was named as A. In order to obtain different F and N doping level TiO_2 materials, another solution comprised of 20 mL ethanol and various amount of NH_4F (the molar ratio of TiO_2/NH_4F is 0.5, 1.0, 1.5 and 2.0, respectively) was named as B. Under vigorous stirring, the solution B and 1.5 mL deionized water was added dropwise within 10 min into solution A. After a further 20 min stirring, the formed mixture was transferred into a Teflon-lined autoclave and heated at 120 °C for 24 h. Then the autoclave was taken out from the oven and cooled to room temperature naturally. The as-fabricated products collected out, washed with ethanol and deionized water, respectively, and then dried in an oven at 80 °C for 12 h. Next, the resulting light yellow material was annealed at 450 °C for 3 h in air to obtain the final F-N co-doped TiO_2. The samples with different starting TiO_2/NH_4F molar ratios of 0.5, 1.0, 1.5 and 2.0 were denoted as TONF-1, TONF-2, TONF-3 and TONF-4, respectively.

2.2. Characterization

Fourier transform infra red (FT-IR) spectra were carried out Bruker Vertex-70 by diffused reflectance accessory technique. Laser Raman spectra were obtained using a Perkin-Elmer Ramanstation 400F Raman spectrometer. The X-ray photoelectron spectroscopy (XPS) measurements were carried out using a Perkin-Elmer RBD upgraded PHI-5000C ESCA system with monochromatic Mg Kα excitation and a charge neutralizer. All bonding energies were calibrated to the C 1s peak at 284.8 eV of the surface adventitious carbon. The crystalline structure and crystallite size of the resulting F-N co-doped TiO_2 materials were determined using X-ray diffraction with a Philips X' PeRT Pro Alpha 1 diffractometer with Cu Kα radiation (λ = 1.5406 Å) operated at a tube current of 40 mA and a voltage of 45 kV. Data were collected over 2θ values from 10° to 80°, at a scan speed of 1° min^{-1}. The geometry and morphology of the co-doped TiO_2 materials were investigated by JSM840F scanning electron microscopy (SEM). The BET specific surface area and pore volume of F-N co-doped TiO_2 samples were determined by a N_2 physisorption technique. UV–vis diffuse reflectance spectra were recorded in a Perkin Elmer Lambda 750S UV/vis spectrometer equipped with an integrated sphere. The electron spin resonant (ESR) spectra were recorded on a Bruker X-band EMX spectrometer operating at 100 kHz field modulation and 1 mW microwave power and equipped with a high-sensitivity cavity (ER4119HS). For the ESR spectra, the samples were directly loaded in the ESR sample tube without further treatment, spectra were recorded on powder samples under liquid nitrogen atmosphere at 130 K and then at room temperature. The g values were determined by reference to a DPPH standard. Computer simulation of the ESR spectrum was obtained using the EasySpin program.

2.3. Photocatalytic reaction

The photocatalytic activities of F-N co-doped TiO_2 samples were tested with methylene blue decomposition under visible light irradiation. The photocatalytic reactions were carried out in an open reactor with a cooling-water-cycle system keeping the reaction temperature constant. The optical system used for the reaction consisted of a 300 W Xenon lamp (Trusttech, Beijing, China) equipped with a 400 nm cut-off glass filter before the output of light source to remove all incoming wavelengths shorter than 400 nm and admit only visible light to enter into the reactor. In each photocatalytic experiment, 100 mg of F-N co-doped TiO_2 catalyst was added in 100 mL of MB solution to form the reaction suspensions. Before the photoreaction, the suspension was stirred in the dark for 240 min to make sure the mixture had achieved adsorption/desorption equilibrium, then 3 mL of the solution was taken from the reactor in a constant time, the sample powder was separated from the solution by a centrifugation method. The MB concentration of the remaining transparent liquid determined from its characteristics absorption peak at 664 nm was analyzed using a UV–vis spectrophotometer. It should be noted that no sacrificial agent and oxygen were added into the solution during the reaction process.

3. Results and discussion

Fig. 1 shows the FT-IR spectra of the F-N co-doped TiO_2, including undoped TiO_2, used here as a reference. It can be seen that all co-doped and undoped TiO_2 samples exhibit absorbance band around 700 cm^{-1}, which can be assigned to the vibration of Ti—O stretching and Ti—O—Ti bridging stretching modes [23]. In comparison with the undoped TiO_2 sample, the F-N co-doped TiO_2 displays additional one absorbance peak located at around 929 cm^{-1}, and this peak corresponds to the Ti—F vibration modes [24], which clearly indicates that the F atom has been incorporated into TiO_2 lattice under solvothermal conditions. However, no evidence for the vibration of N—Ti or N—Ti—N bonds was found in the FT-IR spectra of co-doping samples, this may be due to only a small quantity of N atom incorporating into TiO_2, and the FT-IR cannot detect the minor changes of co-doped sample. The FT-IR technique was usually used to analyze the influence of F-N co-doping on the surface —OH group of TiO_2. As shown in Fig. 1, the FT-IR spectra reveal that the co-doped TiO_2 samples display two peaks around 3400 and 1630 cm^{-1}, which can be ascribed to the stretching vibration of

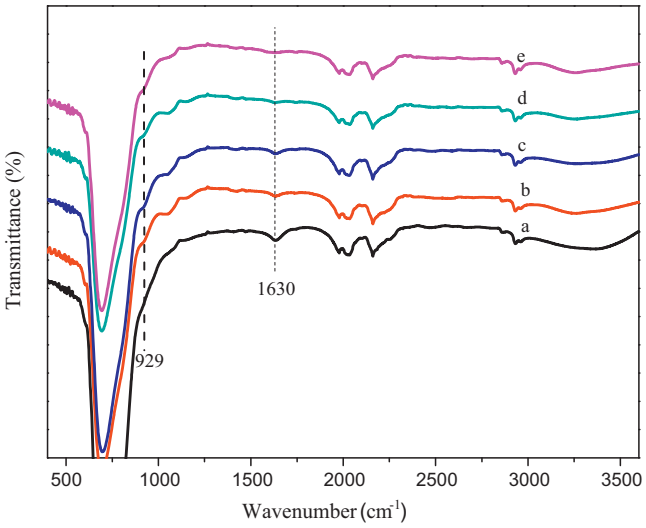

Fig. 1. FT-IR of the F-N co-doped TiO_2 samples. (a) Undoped TiO_2, (b) TONF-1, (c) TONF-2, (d) TONF-3, and (e) TONF-4.

surface —OH group or absorbed water molecules [24,25]. It has been well-accepted that the concentration of —OH group play a vital role in the photocatalytic reaction because the —OH group can capture the photogenerated holes (h^+) and produce to •OH radicals, which are the main reactive species for the degradation of organic compounds [26,27]. In addition, three peaks were seen at 1978 cm^{-1}, 2036 cm^{-1} and 2160 cm^{-1}, which can be assigned to the stretching vibration of C—O, maybe due to the oxidation of existing C element when the products exposed to air.

The surface composition of the F-N co-doped TiO_2 samples was analyzed using XPS. Fig. 2(a) gives the whole XPS survey spectrum of TONF-2 sample, which shows that this sample contains predominantly Ti, O, C, F and N elements. Among these elements, the C1s XPS peak located at around 285 eV is mainly ascribed to adventitious carbon-based contaminant existed in the XPS instrument [28]. Fig. 2(b) shows the high-resolution XPS spectrum of F1s over the co-doped TiO_2. It can be observed that there are two isolated peaks appeared at 689.3 and 696.6 eV in the XPS spectrum of F1s, suggesting two independent environments for F within TONF-2. The low binding energy (BE) of around 689.3 eV can be attributed to the substitution of F atom for O atom in the lattice of TiO_2, as a consequence of forming Ti—F bonds [24]. This finding is consistent with the result of FT-IR spectra. The high BE of 696.6 eV is characteristic of an F atom adsorbed to TiO_2 [29], and this species does not affect the energy band gap of TiO_2. Due to the similar atomic radii between F^- and O^{2-}, the substituted F atom could easily occupy oxygen site in the TiO_2 lattice, and therefore a relatively stronger peak of Ti—F bond was observed in Fig. 2(b), which suggests that a large number of F atoms have been doped into TiO_2. In Fig. 2(c), we show the high-resolution N1s XPS spectrum of TONF-2 sample. It can be observed that there are three weak XPS peaks located at 399.3, 401.6 and 405.4 eV, respectively, indicating three different types of N chemical state within TONF-2 sample. The observation of N 1s at 399.3 eV is mainly attributed to nitrogen in the TiO_2 lattice as O—Ti—N [30], and the peak located at around 401.6 eV corresponds to the nitrogen in the form of a Ti—N—O linkage [31], which are in agreement with previous studies. The peak at around 405.4 is due to the nitrogen species bound to various surface oxygen sites (such as NO or NO_2 molecules) [31,32]. In addition, the relative atomic concentrations of the N and F in TONF-2 sample were investigated based on analysis of XPS data, and the value of N and F atomic concentration were found to be 0.98 and 6.23 at.%, respectively.

Table 1
Pore volume, BET surface area, phase composition and crystalline size of F-N co-doped TiO_2 and undoped TiO_2 samples.

Sample	Pore volume (cm^3/g)	S_{BET} (m^2/g)	Phase composition	Crystalline size (nm)
TiO_2	0.38	40.5	Anatase	33.0
TONF-1	0.46	46.7	Anatase	15.2
TONF-2	0.67	81.2	Anatase	16.9
TONF-3	0.47	55.8	Anatase	17.4
TONF-4	0.44	51.9	Anatase	19.1

Fig. 3 shows the XRD patterns of TONF-1, TONF-2, TONF-3 and TONF-4 samples, respectively, which are all annealed at 450 °C for 3 h in air. It can be seen that the F-N co-doped TiO_2 photocatalysts after high thermal treatment showed only characteristic Bragg diffractions of antanse TiO_2 (JCPDS no. 71-1168) and that there are no significant differences between the four samples. No new diffraction peaks due to N or F containing phase were observed, suggesting these F and N species are either highly dispersed on TiO_2 or under the detection limit of XRD. The average crystal size of the as-prepared samples was calculated using Scherrer equation: $d = 0.9\lambda/b(2\theta)\cos\theta$, where d is the average crystallite size of the co-doped powder sample in nanometer, $b(2\theta)$ is the width of the strongest XRD peak of anatase (1 0 1) TiO_2 at half peak-height in radian (FWHM), λ is the wavelength (nm) of the monochromatic X-ray beam, and 2θ is the angle between the incident and diffracted beams in degree. The calculation result shows that the average crystalline sizes are 15.2, 16.9, 17.4 and 19.1 nm for TONF-1, TONF-2, TONF-3 and TONF-4, respectively. Interestingly, with the increase of the nominal F and N dopant content, a slight increase in the crystalline size over the co-doped samples is observed, this phenomenon was also reported by Giannakas et al. [21] It is worthy noting that crystalline sizes of F-N co-doped TiO_2 in the present work are much smaller than that of reference of TiO_2 sample (33 nm). In addition, it can be seen from Fig. 3 that the intensity of TONF-1 and TONF-4 diffraction peaks is much higher than that of TONF-2 and TONF-3 samples, indicating that the level of fluorine and nitrogen co-doping has a significant effect on the crystallization degree of TiO_2 during the doping process.

To further investigate the crystal structure change of the as-prepared photocatalysts during the F-N co-doping process, Raman spectra were collected from the obtained TONF-1, TONF-2, TONF-3 and TONF-4 samples. As shown in Fig. 4, all the co-doped TiO_2 catalysts annealed at 450 °C present five well-defined Raman modes at around 144, 197, 396, 516 and 639 cm^{-1}, which correspond to the E_g, E_g, B_{1g}, A_{1g} and E_g Raman bands, respectively, and these bands are characteristics of pure anatase structure [33], with no Raman bands due to the impurity phase. This is in accordance with the results of the X-ray diffraction measurements.

Fig. 5 shows the typical micro-surface structures and morphology of the as-fabricated F-N co-doped TiO_2. It shows that the TONF-2 sample presents a shape of agglomerate and some uniform particles are dispersed uniformly on the catalyst surface, indicating that the agglomerate particle is composed of a large quantity of solid structure. These small particles of F-N co-doped TiO_2 could provide more reactive sites for the adsorption of reactants, which can improve the photocatalytic activity of co-doped TiO_2. The above result can be further confirmed by BET analysis. Table 1 lists the textured properties of the co-doped and pure TiO_2 samples. The specific surface area of TONF-1, TONF-2, TONF-3, TONF-4 and TiO_2 are 46.7, 81.2, 55.8, 51.9 and 40.5, respectively. It is clear that the TONF-2 catalyst possesses larger surface area among all the as-prepared samples.

The UV–vis diffuse reflectance spectra (DRS) were used to determine the effects of F-N co-doping on the light absorption of TONF samples. Fig. 6 shows the UV–vis DRS spectra of the F-N co-doped

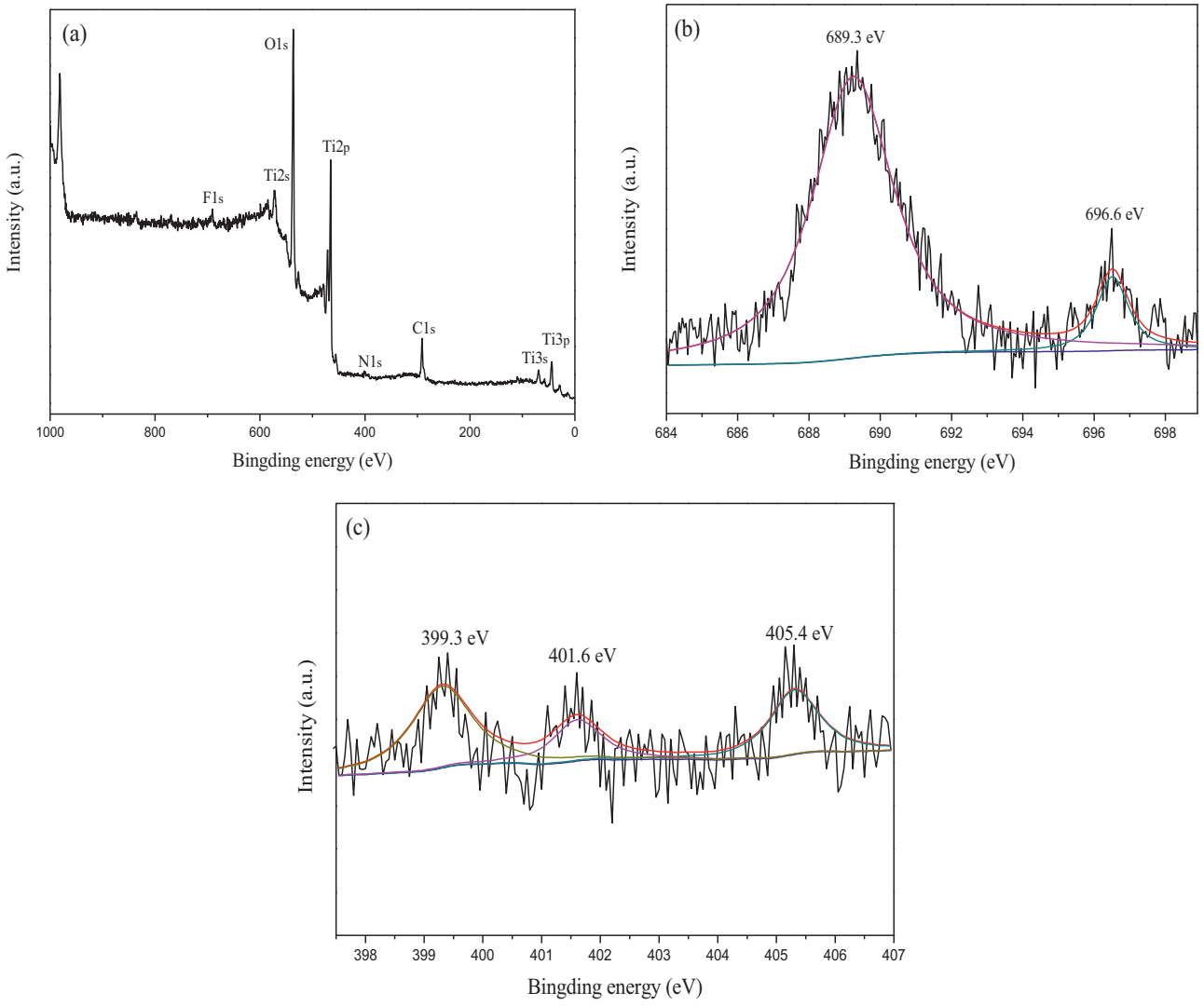

Fig. 2. The XPS spectra of TONF-2 sample, (a) the whole survey spectrum, (b) F1s XPS spectrum and (c) N1s XPS spectrum.

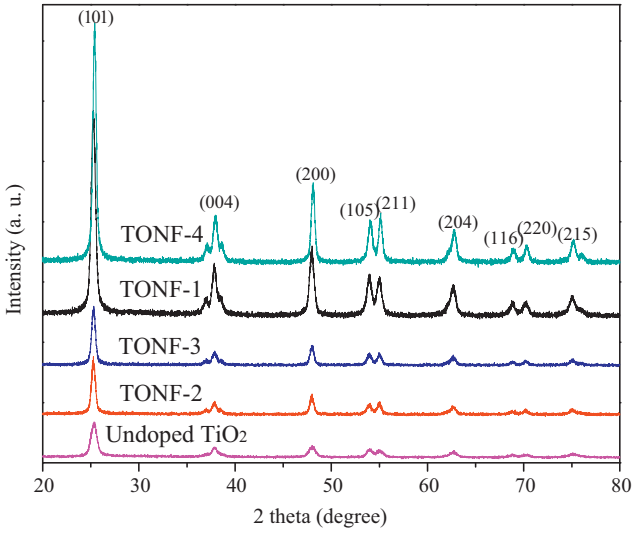

Fig. 3. XRD patterns of F-N co-doped TiO_2 samples and undoped TiO_2.

TiO_2 and the undoped TiO_2 samples. As shown, the undoped TiO_2 sample depicts a strong and broad absorption feature in the UV region due to the inter band electronic transitions. In comparison with undoped TiO_2, all of F-N co-doped samples show a similar light absorption band and have apparent absorption in the visible region from 390 nm to 535 nm. Particularly, TONF-2 sample has two optical absorption thresholds at 535 and 415 nm in UV–visible spectrum, which corresponds to band gaps of 2.32 eV and 2.99 eV, respectively. Light absorbance features of the co-doped samples suggest that the F and N were co-doped into TiO_2 lattice and altered their energy band gap. However, as previously reported [34], when TiO_2 is doped with F atoms only, it does not cause a red-shift in the fundamental absorption edge of TiO_2, because the F atoms doping leads to forming localized level with high density below the valence band of TiO_2. It is therefore inferred that the visible light absorption of TONF samples appeared in UV–visible spectrum arises from the results of doping nitrogen and/or the other species created by co-doping. In this study, the origin of visible light absorption can be explained by the following two factors. Firstly, it is known that nitrogen substitutes some oxygen atoms in the lattice generating an N midgap level above the O2p valence band, which narrows the band gap of TiO_2 and consequently induces a visible light absorption. Furthermore, even though fluorine dopant does not directly improve the absorption of TiO_2 toward visible light, it

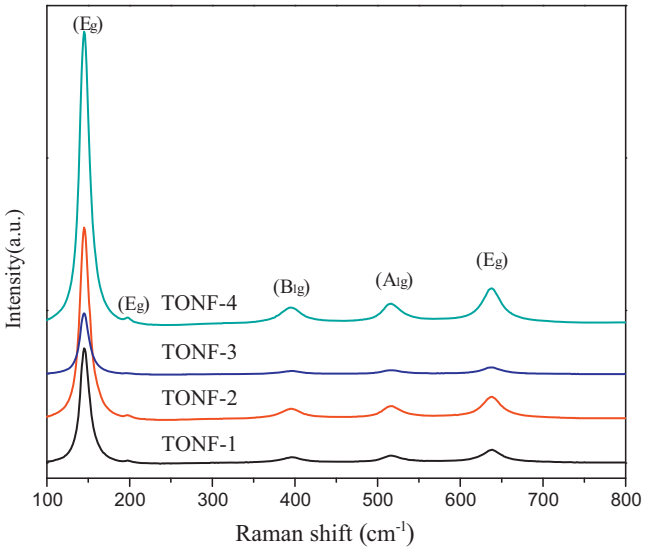

Fig. 4. Raman spectra of F-N co-doped TiO_2 samples.

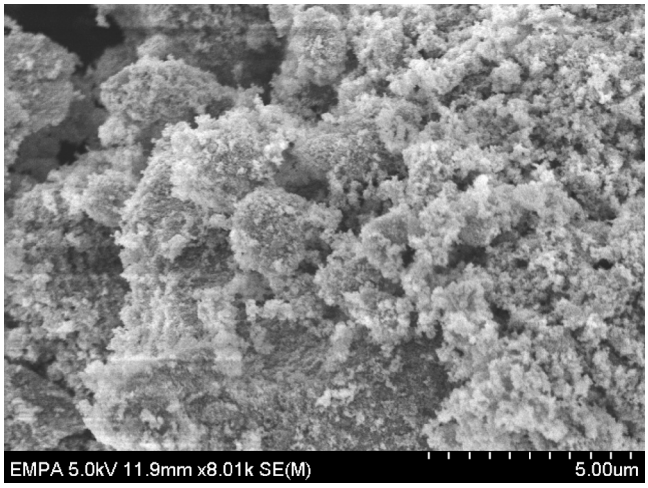

Fig. 5. The representative SEM image of the TONF-2 sample.

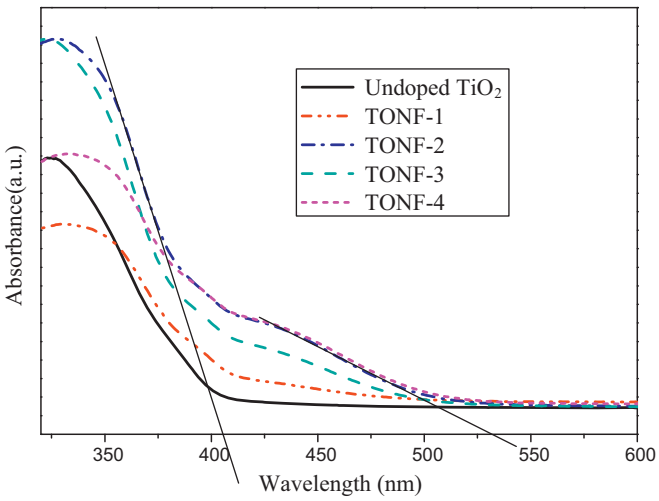

Fig. 6. UV–vis diffuse reflectance spectra of the undoped TiO_2 and F-N co-doped TiO_2.

Table 2
Spin Hamiltonian parameters of species identified by EPR.

Species	g_1	g_2	g_3
$O_2^{\bullet-}$	2.011	2.001	1.974
Ti^{3+}	1.999	1.993	1.954

contributes to promote the creation of Ti^{3+} ions and oxygen vacancies in the bulk or over the surface of TiO_2 and in this way induce an ESR signal and visible light absorption [35], which will be discussed later.

Low temperature and room temperature electron spin resonant (ESR) spectra were recorded to investigate the change of the crystal lattice structure and the paramagnetic centers present in F-N co-doped TiO_2. Fig. 7 shows the experimental ESR spectra of TONF-2 sample recorded at various temperatures, along with the corresponding computer simulation of the ESR spectra, and the g tensors used to conduct the simulated spectra are summarized in Table 2. Noted that the ESR spectra have been used as a reference data in our previous reported work [24], but which does not lucubrate. As shown in Fig. 7(a), it can be seen that the ESR spectra

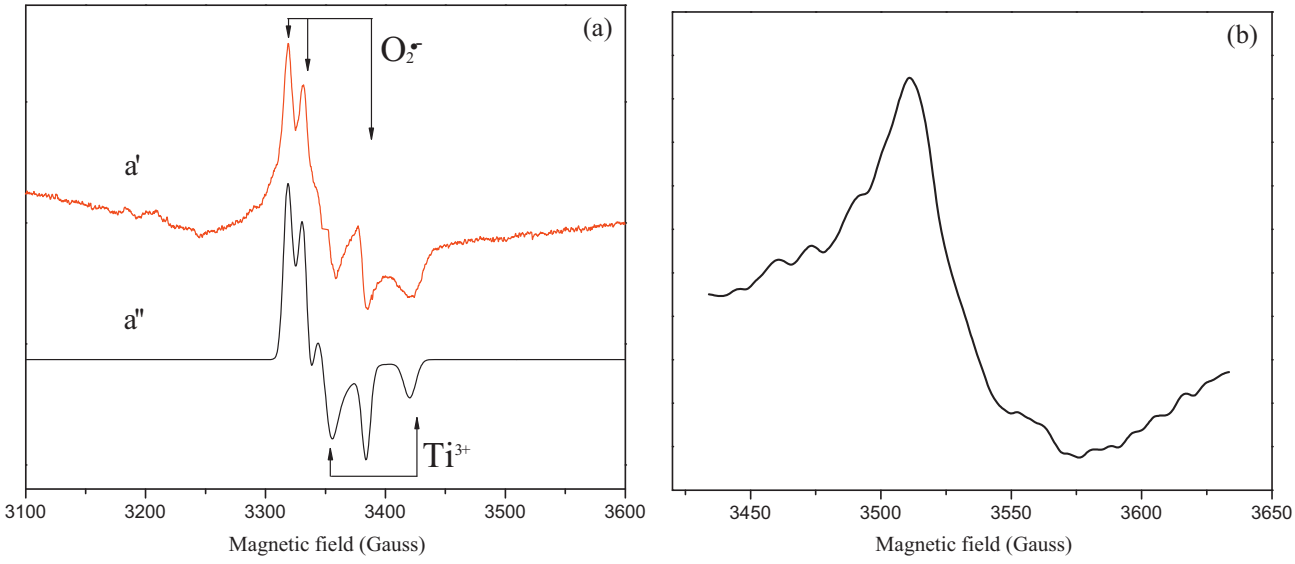

Fig. 7. ESR spectra and corresponding simulation of TONF-2: (a) recorded at 130 K (a′ experimental spectrum; a″ computer simulation); (b) recorded at room temperature.

recorded at 130 K shows significant difference in comparison with that recorded at room temperature, and the results of computer simulation indicate that two distinct paramagnetic species exist in the crystal lattice structure of TiO_2 when the ESR experiment performed at 130 K. The signal with g values of $g_1 = 2.011$, $g_2 = 2.001$ and $g_3 = 1.974$ is known to be $O_2^{\bullet -}$ (superoxide radical) [34,36], formed by photogenerated holes trapped by superoxide ions. While the simulation for the second paramagnetic signal with g values of $g_1 = 1.999$, $g_2 = 1.993$ and $g_3 = 1.954$ can be assigned to the Ti^{3+} ions in the anatase lattice generated by photoelectron capture [27,37]. This is consistent with the previous reports that the substitution of O atom by F atom during the solvothermal process could induce the formation of Ti^{3+} ions and oxygen vacancies ($V_O^{\bullet}$), and F-N co-doping could further improve the Ti^{3+} and $V_O^{\bullet}$ quantity [38]. As shown in Fig. 7(b), the ESR spectrum recorded at room temperature only shows a broad signal, and its g factors at approximately 2.004 can be assigned to the characteristic of paramagnetic materials containing "F-centers" or $V_O^{\bullet}$ [11,24,27]. This ESR peak could be attributed to the single-electron trapped on $V_O^{\bullet}$ sites and which is caused a magnetic resonance detected by ESR. Besides, the signal related to Ti^{3+} ions was not observed in Fig. 7(b), and this is similar to the results observed in recent studies: Bianchi et al. [39] reported that the Ti^{3+} ions are characterized by very short relaxation time, so their ESR resonances can be detected at very low temperature only, as the recombination rate of electron–hole is significantly reduced at low temperature. In addition, the N containing species (normally labeled as $N_b^{\bullet}$) which already reported in many studies was not detected by low temperature and room temperature ESR, which can be explained by a reversible electron transfer between the 3d orbital of the Ti^{3+} ions and the paramagnetic N centers [40,41].

According to the above results of ESR data, it can be found that the F and N co-doping favors the formation of lattice Ti^{3+} ions and $V_O^{\bullet}$ sites in the bulk and surface of TiO_2, and these paramagnetic centers as well as the N dopant can give an obvious change in the band edge position of TiO_2. As shown in Fig. 6, the band thresholds position of TONF-2 shifts to 2.99 eV, and a shoulder with an edge at 2.32 eV is observed, indicating that the F-N co-doping has a significant effect on the electronic band structure of TiO_2.

In order to better understand the effect on the TiO_2 band gap by co-doping processes, we attempt to illuminate the mechanisms of visible-light-responsive activity of F-N co-doped TiO_2 based on our experimental data. A lot of researchers have confirmed that an excess electron in the lattice could reduce Ti^{4+} to produce Ti^{3+} species($Ti^{4+} \rightarrow Ti^{3+}$) [31], and these Ti^{3+} species observed by ESR spectroscopy can lead to formation of an isolated defect energy level below the bottom of the conduction band (CB) of TiO_2, meanwhile, the $V_O^{\bullet}$ formed due to F-N co-doping will lead to another energy level which is also under CB of TiO_2. As a result, the formation of Ti^{3+} and $V_O^{\bullet}$ defect energy levels would overlap each other and finally form a broad defect energy state belt in the band gap of TiO_2. Moreover, when N was introduced into TiO_2 lattice, an N2p midgap state can be formed above the top of valence band (VB) of TiO_2. On the basis of the discussion afore, the schematic illustration of the electronic band structure was given in Fig. 8, while the separation process of photogenerated electrons and holes was also shown in Fig. 8. It clearly reveals that the narrowing of the electronic band gap of F-N co-doped TiO_2 catalysts is a synergetic result of the existed defect energy state belt related to Ti^{3+} and $V_O^{\bullet}$ and the N2p midgap state. It should be noted that these energy levels not only enhance the visible light absorption but also serve to trap the photogenerated electron, with consequent improvement of the charge separation efficiency and quantum efficiency for F-N co-doped TiO_2.

Fig. 9 shows the UV–vis spectra of MB solution before and after visible light irradiation for different exposure periods in the presence of the TONF-2 sample. The characteristic absorption band of

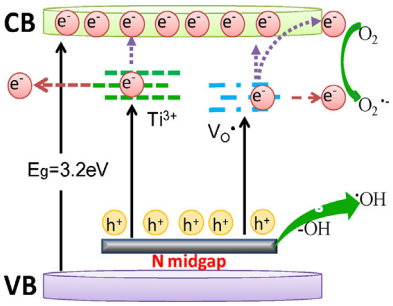

Fig. 8. The schematic illustration of the electronic band structure and the separation of photogenerated electrons and holes under visible light irradiation ($V_O^{\bullet}$: oxygen vacancies).

MB at 664 nm diminished quickly, accompanied by slight concomitant blue-shift from 664 to 600 nm of the maximum absorption with the increasing visible light irradiation time. The intensity of the MB characteristic band is closed to 0 after 210 min photoreaction, indicating that the model dye has been completely decolorized.

Fig. 10 shows the visible-light-induced photocatalytic decomposition of MB solution over the F-N co-doped TiO_2 photocatalysts.

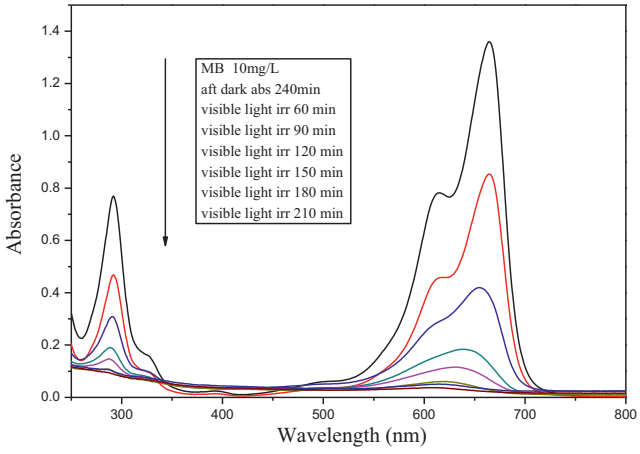

Fig. 9. UV–vis spectra of a 10 ppm MB solution before and after visible light irradiation for different times in the presence of the TONF-2 sample.

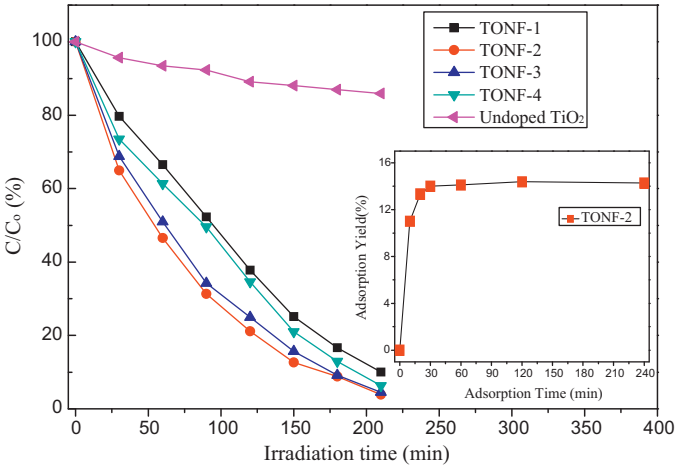

Fig. 10. Photocatalytic degradation of methylene blue (MB) over F-N co-doped TiO_2 samples under visible light irradiation ($\lambda > 400$ nm), and the inset is MB adsorption curves of TONF-2 sample (reaction conditions: $C_o = 10$ ppm, Catalyst loading: 1 g/L).

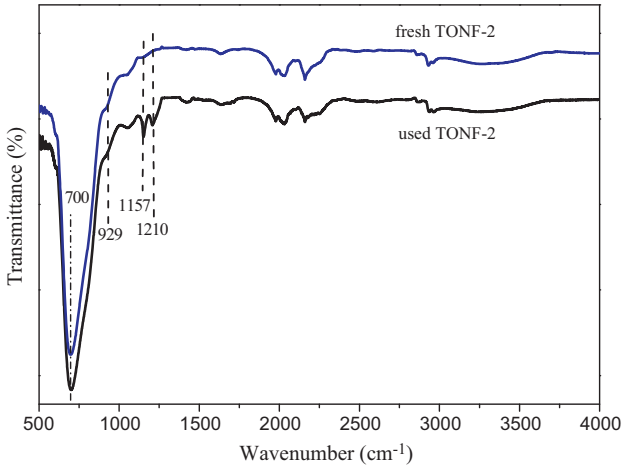

Fig. 11. the FT-IR spectra of TONF-2 sample before and after the photocatalytic reaction.

For comparison, the results of degradation of MB over the undoped TiO_2 were also given in Fig. 10. It can be seen that the nominal doping amount of starting NH_4F precursor affects the photocatalytic activity. Among them, the TONF-2 sample showed the highest photodegeadation activity with a MB conversion of 96% after 210 min irradiation, while the TONF-1 showed a relatively lower photocatalytic activity. Due to its big energy band gap (3.2 eV), the undoped TiO_2 could not be activated by visible lights. However, a slight photodegradation of MB on the undoped TiO_2 was observed, which can be attributed to the dye-sensitizing effect. The inset of Fig. 10 shows the MB adsorption curves over TONF-2 sample. It is clear that the co-doped sample completely reached adsorption equilibrium within 30 min, and the adsorption yield of MB solution is about 14% for TONF-2 catalyst.

As mentioned above, fluorine and nitrogen co-doping could produce several beneficial effects for the preparation of visible-light-responsive TiO_2 photocatalysts. (i) The presence of N species in the band gap of TiO_2 can generate N2p midgap on the top of valence band. (ii) The creation of $V_O^{\bullet}$ sites and the formation of Ti^{3+} ions could form some isolated defect energy level and therefore decrease the conduction band energy level of TiO_2. (iii) The surface-absorbed oxygen at $V_O^{\bullet}$ sites was active for the formation of the $O_2^{\bullet-}$ radicals, which were detected by ESR. Based on the above beneficial effects, we tentatively concluded that the enhanced visible light photocatalytic activities of the as-prepared photocatalysts are mainly ascribed to F and N incorporated into the lattice of TiO_2. The creation of N impurity, Ti^{3+} ions and $V_O^{\bullet}$ sites in TiO_2 energy gap induced by co-doping process are important factors for efficient narrowing of band gap and inducing visible light absorption. Nevertheless, the contributions of these Ti^{3+} ions and oxygen vacancies not only cause the optical absorption, but also act as active sites to trap the photogenerated electrons and hinder the recombination of electrons and holes in photodegradation of MB. On the other hand, the FT-IR analysis shows that F and N co-doping could enrich the surface —OH groups over TiO_2, whilst the ESR data indicates that there are a large number of $O_2^{\bullet-}$ radicals formed on the surface of TONF-2 sample. As a result, both of the active species could attack the organic compound and greatly enhance the activity of photocatalytic degradation [42].

In order to investigate the influence of photodegradation experiment on the crystal structure and the functional group over the surface of co-doped TiO_2, FT-IR spectra of TONF-2 before and after the photoreactions were collected using Bruker Vertex-70 FT-IR spectrometer and the results were given in Fig. 11. In comparison with the fresh TONF-2 sample, the FT-IR spectra of the used TONF-2 sample shows that the peaks due to the stretching vibrations of the Ti—O—Ti bonds and Ti—F vibration modes remains existed after 210 min photoreaction. In addition, the peak intensity of Ti—O—Ti and Ti—F bonds for the fresh and used samples are almost similar to each other, indicating a well crystallized anatase structure and excellent durability of our F-N co-doped TiO_2 catalyst. Furthermore, it is found that the FT-IR bands corresponding to —OH group (3400 cm^{-1}) and absorbed water molecules (1630 cm^{-1}) on the used TONF-2 sample became much weaker after the photoreaction, which suggests that the surface —OH groups as the major reactive species play a vital role in the decomposition of organic molecule. The FT-IR spectra also reveal that the used TONF-2 sample displays two additional absorbance peaks around 1157 and 1210 cm^{-1} indicative of the vibration of C—O—C bond, which was produced by the photodegradation MB experiment.

4. Conclusions

We developed a simple ethanol–water solvothermal method to synthesize nano-structured F-N co-doped TiO_2 photocatalysts. The UV–vis DRS spectra showed that all the prepared samples exhibited a shift of the absorption edge toward to visible light region, and the XPS data showed that F and N atoms have been incorporated into TiO_2 lattice, and the N dopant existing in the energy gap could form N midgap. Further, the ESR analysis revealed that both F and N ions favor formation of lattice Ti^{3+} paramagnetic center and oxygen vacancies in F-N co-doped solid.

The obtained F-N co-doped TiO_2 samples displayed higher photocatalytic activity in clean-up of MB dye under visible light irradiation, and the superior visible-light-responsive photoactivity of F-N co-doped TiO_2 can be attributed to the narrow band gap through the existed Ti^{3+} ions, $V_O^{\bullet}$ sites and the N2p midgap state in TiO_2.

Acknowledgements

This work was financially supported by the National Natural Science Foundation of China (Grant No. 21303130), the Fundamental Research Funds for the Central Universities (Grant No. 2012jdhz40), and the Overall Scientific and Technological Innovation Program of Shaanxi Province of China (No. 2012KTCL01-09).

References

[1] K. Vinodgopal, D.E. Wynkoop, Environ. Sci. Technol. 30 (1996) 1660–1666.
[2] B.H. Diya'uddeen, W.M.A.W. Daud, A.R. Abdul Aziz, Process. Saf. Environ. Prot. 89 (2011) 95–105.
[3] G. Yang, Z. Yan, T. Xiao, Appl. Surf. Sci. 258 (2012) 4016–4022.
[4] A. Fujishima, X. Zhang, D.A. Tryk, Surf. Sci. Rep. 63 (2008) 515–582.
[5] G. Yang, Z. Yan, T. Xiao, B. Yang, J. Alloys Compd. 580 (2013) 15–22.
[6] T.R. Gordon, M. Cargnello, T. Paik, F. Mangolini, R.T. Weber, P. Fornasiero, C.B. Murray, J. Am. Chem. Soc. 134 (2012) 6751–6761.
[7] T. Lv, L. Pan, X. Liu, T. Lu, G. Zhu, Z. Sun, C.Q. Sun, Catal. Sci. Technol. 2 (2012) 754–758.
[8] A.K. Benabbou, Z. Derriche, C. Felix, P. Lejeune, C. Guillard, Appl. Catal. B 76 (2007) 257–263.
[9] J. Ye, W. Liu, J. Cai, S. Chen, X. Zhao, H. Zhou, L. Qi, J. Am. Chem. Soc. 133 (2011) 933–940.
[10] G. Yang, T. Xiao, J. Sloan, G. Li, Z. Yan, Chem. Eur. J. 17 (2011) 1096–1100.
[11] Z. Jiang, L. Kong, F.S. Alenazey, Y. Qian, L. France, T. Xiao, P.P. Edwards, Nanoscale 5 (2013) 5396–5402.
[12] Z. Jin, X. Zhang, G. Lu, S. Li, J. Mol. Catal. A 259 (2006) 275–280.
[13] L.Q. Jing, X.J. Sun, B.F. Xin, B.Q. Wang, W.M. Cai, H.G. Fu, J. Solid State Chem. 177 (2004) 3375–3382.
[14] R. Asahi, T. Morikawa, T. Ohwaki, K. Aoki, Y. Taga, Science 293 (2001) 269.
[15] Y. Huo, Y. Jin, J. Zhu, H. Li, Appl. Catal. B 89 (2009) 543–550.
[16] Y. Su, X. Zhang, M. Zhou, S. Han, L. Lei, J. Photochem. Photobiol. A 194 (2008) 152–160.
[17] J. Bu, J. Fang, F. Shi, Z. Jiang, W. Huang, Chinese J. Chem. Phys. 23 (2010) 95–101.
[18] G. Yang, Z. Yan, T. Xiao, Appl. Surf. Sci. 258 (2012) 8704–8712.

[19] J. Fang, F. Shi, J. Bu, J. Ding, S. Xu, J. Bao, Y. Ma, Z. Jiang, W. Zhang, C. Gao, W. Huang, J. Phys. Chem. C 114 (2010) 7940–7948.
[20] D. Li, H. Haneda, S. Hishita, N. Ohashi, Chem. Mater. 17 (2005) 2588–2595.
[21] A.E. Giannakas, E. Seristatidou, Y. Deligiannakis, I. Konstantinou, Appl. Catal. B 132/133 (2013) 460–468.
[22] D. Chen, Z. Jiang, J. Geng, J. Zhu, D. Yang, J. Nanopart. Res. 11 (2009) 303–313.
[23] D. Huang, S. Liao, S. Quan, L. Liu, Z. He, J. Wan, W. Zhou, J. Mater. Res. 22 (2007) 2389–2397.
[24] G. Yang, Z. Jiang, H. Shi, M.O. Jones, T. Xiao, P.P. Edwards, Z. Yan, Appl. Catal. B 96 (2010) 458–465.
[25] X. Chen, X. Wang, Y. Hou, J. Huang, L. Wu, X. Fu, J. Catal. 255 (2008) 59–67.
[26] L.-C. Chen, F.-R. Tsai, S.-H. Fang, Y.-C. Ho, Electrochim. Acta 54 (2009) 1304–1311.
[27] F. Fresno, M.D. Hernández-Alonso, D. Tudela, J.M. Coronado, J. Soria, Appl. Catal. B 84 (2008) 598–606.
[28] J. Fang, F. Wang, K. Qian, H. Bao, Z. Jiang, W. Huang, J. Phys. Chem. C 112 (2008) 18150.
[29] L. Ley, M. Cardona, Photoemission in Solid II, Springer, Berlin/Heidelberg, 1979.
[30] M. Pelaez, A.A.D.L. Cruz, E. Stathatos, P. Falaras, D.D. Dionysiou, Catal. Today 144 (2009) 19–25.
[31] G. Yang, Z. Jiang, H. Shi, T. Xiao, Z. Yan, J. Mater. Chem. 20 (2010) 5301–5309.
[32] M. Mrowetz, W. Balcerski, J. Colussi, M.R. Hoffmann, J. Phys. Chem. B 108 (2004) 17269–17273.
[33] K. Yanagisawa, J. Ovenstone, J. Phys. Chem. B 103 (1999) 7781–7787.
[34] E.A. Reyes-Garcia, Y. Sun, K.R. Reyes-Gil, D. Raftery, Solid State Nucl. Magn. Reson. 35 (2009) 78.
[35] W. Wang, C. Lu, Y. Ni, M. Su, Z. Xu, Appl. Catal. B 127 (2012) 28–35.
[36] J. Soria, J. Sanz, I. Sobrados, J.M. Coronado, F. Fresno, M.D. Hernandez-Alonso, Catal. Today 129 (2007) 240–246.
[37] C. Di Valentin, E. Finazzi, G. Pacchioni, A. Selloni, S. Livraghi, A.M. Czoska, M.C. Paganini, E. Giamello, Chem. Mater. 20 (2008) 3713.
[38] A.M. Czoska, S. Livraghi, M. Chiesa, E. Giamello, S. Agnoli, G. Granozzi, E. Finazzi, C.D. Valentin, G. Pacchioni, J. Phys. Chem. C 112 (2008) 8951–8956.
[39] C.L. Bianchi, G. Cappelletti, S. Ardizzone, S. Gialanella, A. Naldoni, C. Oliva, C. Pirola, Catal. Today 144 (2009) 31–36.
[40] S. Livraghi, M.C. Paganini, E. Giamello, A. Selloni, C. Di Valentin, G. Pacchioni, J. Am. Chem. Soc. 128 (2006) 15666–15671.
[41] F. Napoli, M. Chiesa, S. Livraghi, E. Giamello, S. Agnoli, G. Granozzi, G. Pacchioni, C. Di Valentin, Chem. Phys. Lett. 477 (2009) 135–138.
[42] G. Yang, B. Yang, T. Xiao, Z. Yan, Appl. Surf. Sci. 283 (2013) 402–410.